JOURNAL OF MATERIALS SCIENCE **36** (2001) 1747–1753

Nanoscale mechanical degradation of titanium/PETI-5 adhesive interface due to thermal exposure

J. D. HOLBERY*,‡, R. M. FISHER
Department of Materials Science and Engineering, University of Washington, Seattle, WA 98195 USA
E-mail: james.holbery@csem.ch

Titanium substrates coated with silicate/zirconate sol-gel and plasma sputtered chromium have been adhered using a combined PETI-5 polyimide psuedo-thermoplastic primer/adhesive system. Composite laminates were exposed to thermal aging up to 2000 hours at 194°C, subsequently interface analysis was performed using nanoindentation to determine material modulus degradation and plastic deformation changes. Inhomogeneities at the interface mandated that both low loads (as low as 25 μN) and a 90° cube-corner diamond tip be utilized to obtain sub-micron resolution. Sol-gel coated and chromium coated titanium substrates exhibited a pronounced step-wise gradient across the interface dependent upon the indent load level and corresponding depth. Thermal aging produced an increase in both the PETI-5 primer and adhesive modulus by 20% and upwards of 30%, respectively. Sol-gel modulus increased by approximately 15% with environmental exposure and at an exposure level at 1000 hours, the chromium modulus increased approximately 20%. An decrease in plastic deformation resulting from thermal aging observed and reported, combined with material modulus alteration, is thought to be critical in predicting the overall life in adhesion joints within mission critical aerospace structures.

1. Introduction

1.1. General

The High Speed Civil Transport (HSCT), a research program directed by NASA, proposes an air speed capability of Mach 2.4 combined with an operating temperature of 177°C. The operating environment is more severe than conventional subsonic air transport vehicles due to high temperatures associated with the aerodynamic friction heating caused by supersonic cruise speeds. In addition, the fraction of the operating empty weight for a supersonic airframe structure is significantly less as compared to conventional subsonic commercial vehicles requiring the use of innovative structural concepts and advanced materials to satisfy stringent weight requirements. Bonded Titanium structures are a design consideration for the HCST due to the ability to achieve high structural efficiency achievable with structural bonding.

PETI-5, a patented polyimide resin developed at NASA Langley to offer high toughness and thermo-oxidative stability for long-term structural applications at elevated temperatures, has been the basis for composite resins and adhesives considered for bonding applications on the HSCT [1, 2]. The adhesive is applied in conjunction with PETI-5 primer (Cytec Fiberite BR × 5), a dilute solution of the NASA LaRC PETI-5 polyimide with additives for handling purposes applied at a thickness ranging from 100–200 nm [3].

Titanium alloys considered in this study are Ti-6Al-4V (Ti-6-4) and Ti-15V-3Cr-3Al-3Sn (Ti-15-3-3-3). While Ti-6-4 is widely used in the annealed form with a Ultimate Tensile Strength (UTS) of 895 Mpa, Ti-15-3-3-3 is a beta alloy developed to be cold-formable yet heat treatable to achieve a UTS above 1 Gpa.

Two coatings have been selected as potential gradient materials between the metallic substrate and organic resin; a combination silicate/zirconate sol-gel and a plasma sputtered chromium. Substrates have been prepared prior to sol-gel application by conventional grit blasting followed by a nitric/HF acid etch. The aliphatic sol-gel coating is formed by creating a low-concentration solution of aminopropyltrimethoxysilane (APS) and zirconium n-propoxide in water. The pH conditions are manipulated to cause the APS and zirconate to hydrolyze and partially polymerize. The solution is applied to the titanium substrate and allowed to air dry. It is then baked at 125°C to initiate the hydrolyzed silane and zirconate to undergo a condensation

* Author to whom all correspondence should be addressed.
‡ *Present Address*: CSEM Instruments SA, Neuchatel, Switzerland.

reaction and form a mixed organic/inorganic matrix with covalent bonds to the titanium oxide substrate. The goal of this process is to completely remove the hydroxide groups, leaving only the amine organic functionality reacting the amine with the polyamic acid primer to form a direct chain of covalent bonds between the adhesive and titanium substrate.

Chromium is applied to a previously chemically etched Titanium substrate in a high-vacuum atmosphere at a thickness of 1000 Å similar to processes utilized in the microelectronic industry. Prior to sputtering, the titanium substrate is plasma sputtered to remove native titanium oxide rendering a clean metallic titanium surface necessary to achieve a strong stable chromium/titanium bond. This process takes advantage of a unique affinity for chromium oxide that polyimides exhibit. Although the exact method of interaction is the subject of some debate, polyimides, particularly in the amic acid form, bond strongly with chromium coatings.

Several factors affect long-term adhesive stability, although the interfacial region between a polymer and substrate is commonly thought to be critical in predicting system performance. It has been shown that mechanical failure will often occur at the joint after exposure to harsh environmental conditions [4–6]. Physical aging as a result of interface environmental exposure accelerates time-dependent changes in volume, enthalpy, and entropy, as well as decrease in mechanical properties [7, 8]. This physical phenomenon is increased drastically when a large coefficient of thermal expansion in the interface material exists. The combined effects of physical and chemical aging of the systems described herein have been examined and it was found that physical aging begins at the outset of exposure and continues to progress while the effects of chemical aging began with increased exposure time [9]. The present work aims to measure at the interface the nano-mechanical properties of bonded Titanium-PETI-5 adhesive laminates under consideration for structural applications on the HSCT and quantify the nano-mechanical degradation due to thermal aging.

1.2. Nano-mechanical

In these experiments, we utilized a Park Scientific CP atomic force microscope (ThermoMicroscopes, Palo Alto, CA) combined with a Hysitron® Nanoindentation transducer and associated software (Hysitron Inc., Minneapolis, MN) [10]. Instruments mounted on a multilayer vibration pad were situated in a room maintained at $20^{\circ}C \pm 2^{\circ}C$. Contact Atomic Force Microscopy (AFM) images were acquired using a diamond indentation tip with the Park CP in constant-force mode. Additional AFM images were acquired using a Digital Instruments Nanoscope III Atomic Force Microscope (Digital Instruments, Santa Barbara, CA) in both contact and tapping modes.

Nanoindentation analysis based on the elastic contact model was addressed initially by workers at the Baikov Institute of Metallurgy in Moscow during the 1970's [11], the first practical method was presented in 1986 by Doerner and Nix [12] and subsequently refined by Oliver and Pharr [13]. The method is based on the assumptions that Young's modulus of elasticity is independent of indentation depth, deformation upon unloading is purely elastic, and sample compliance and indenter tip may be combined as springs in series [13].

1.3. Indenter tip geometry

Measurements were initially obtained in this study using a Berkovich diamond tip [14]. Imaged indentations indicate a sharp Berkovich tip radius does not produce sufficiently small material impressions to obtain a resolution required to analyze very thin interfaces. This is due to the projected contact area to depth relationship for this tip being described as A_c as follows:

$$A_c = 24.5h_c^2 \tag{1}$$

where h_c is the contact depth.

The actual curvature of this Berkovich tip has been determined using a Field Emission Scanning Electron Microscope (FESEM, Joel Model JSM 630F) and is approximately 150 nm, although it is difficult to determine exact dimensions from the view in Fig. 1a. Recently, one group has reported Berkovich tips with a radius of 23 nm [15]. By comparison, the projected contact area to depth relationship for the 90° cube-corner tip is as follows:

$$A_c = 2.598h_c^2 \tag{2}$$

The radius of the 90° cube-corner tip used was reported to be between 30–50 nm by the manufacturer, though

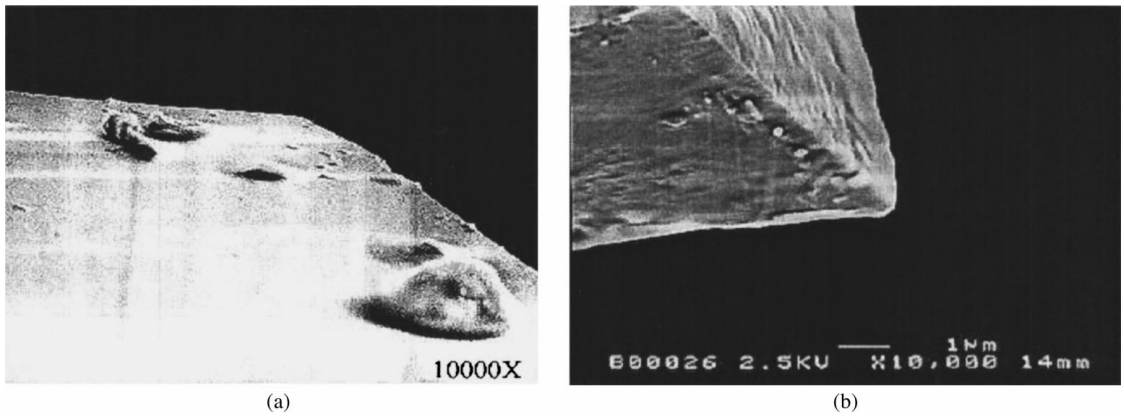

(a) (b)

Figure 1 (a) Three-sided Berkovich with tip radius estimated at 150 nm. (b) 90° Cube Corner tip with radius estimated at 120 nm.

the actual curvature of the tip as determined by FESEM is approximately 100 nm (Fig. 1b). One is able to view a slight imperfection at the tip end corresponding with reports in the literature claiming typical "sharp" cube-corner tip radii are on the order of 100 nm [16].

The output from these measurements result in two principal values: hardness and indentation modulus. Nanoindentation hardness is an average of material properties and is not a fundamental physical quantity.

2. Experimental

2.1. Materials

Laminates of several thin foil and bonded laminate configurations were supplied by the Boeing Company according to geometry, surface treatment, aging, and laminate configurations. Samples were exposed to 204°C thermal aging at ambient atmosphere for time exposure durations of both 1000 and 2000 hours.

2.2. Sample preparation

Sample preparation was modeled after the protocol used within the Boeing Company [17] and the final steps were altered to reflect the atomic scale resolution necessary to perform this research. Samples were rough cut (lap shear samples with a diamond wheel cut-off saw) and cured into solid blocks using epoxy resin (Resin 5, Struers, Westlake, OH) and subsequently a combination of hand sanding and hand polishing was performed to prepare the samples for imaging and nanoindentation.

2.3. Interface characterization

In this study, the adhesion promoting Sol-Gel and Chromium layers were nominally 1000 Å. Sol-gel varies slightly in thickness as a result of the varying concentration gradients and the uneven evaporation rate of the carrier.

Images of a Sol-gel deposited Titanium substrate fractured to partially fail the Sol-gel coating have been acquired with a Scanning Electron Microscope (JOEL 840, Fig. 2). The coating is inherently brittle; as a consequence, when the substrate is bent to approximately 30° failure in the coating is initiated. This sample was bent around a mandrel and subsequently prepared for imaging.

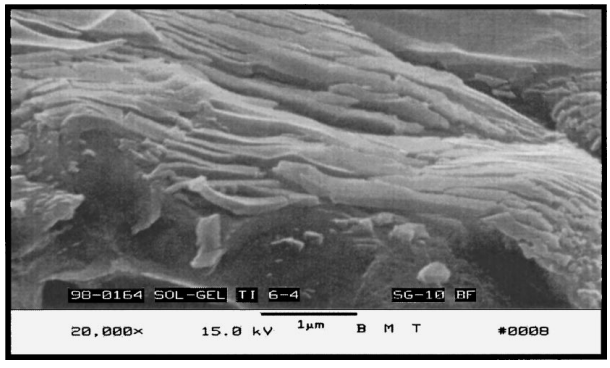

Figure 2 Scanning Electron Microscope image of Titanium/Sol-gel laminate failed to determine Sol-gel thickness.

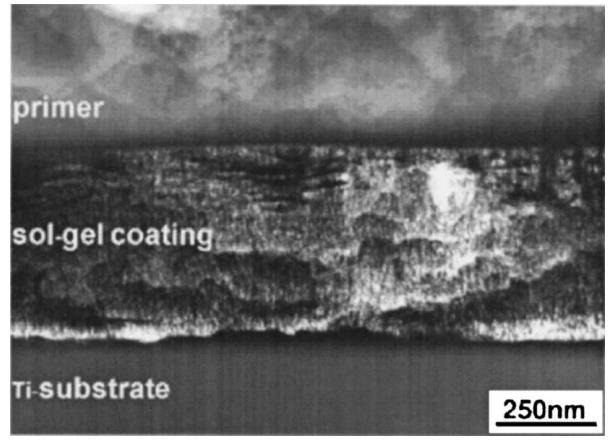

Figure 3 Transmission Electron Microscopy cross-section profile of Titanium/Sol-gel/Primer interface.

Transmission Electron Microscopy (JOEL Model 400) has been used to determine the interface thickness of a Titanium/Sol-gel/Primer with the Sol-gel coating approximately 700 Å in thickness (Fig. 3). While this thickness is adequate to indent provided the radius of the diamond tip is sufficiently small, the inherent roughness of the Titanium substrate (as may be seen in the TEM image) adds to the difficulty of following a relatively straight line of indentation across the interface.

3. Results and discussion

3.1. Nanoindentation standards

Indentation measurements of the sample sets were performed. Low loads combined with the cube-corner tip allow for sample imprints inherently smaller in area as compared to the Berkovich tip, thus providing the ability to measure within several hundred Angstroms and remain a distance 4–5 times the sample imprint in diameter apart. Fig. 4 illustrates a series of chromium interface Load-Displacement plots aged 1000 hours. Corresponding modulus and hardness values for each material tested are listed in Table I. The titanium measurement is characteristic of titanium measurements made on other samples, exhibiting the plastic deformation curve characteristic of work hardened materials. The chromium interface exhibits elastic-plastic behavior that is more pronounced than the primarily elastic sol-gel region. More important is the curve shape of the primer and PETI-5 regions. Clearly in the aged sample the area under the curve is greater and resembles more of a plastic nature than the elastic-plastic depicted in the "As Manufactured" plots. This is most likely due to polymer embrittlement, increased cross-linking or chain length reduction as a result of aging.

TABLE I Measured modulus and hardness values corresponding to curves plotted in Fig. 16 of a Titanium/Sol-gel/Primer/PETI-5 adhesive interface aged for 1000 hours

Material	Modulus (GPa)	Hardness (GPa)
Titanium	181	16.3
Chromium	32.3	1.97
Primer Region	11.9	0.71
PETI-5	7.5	0.43

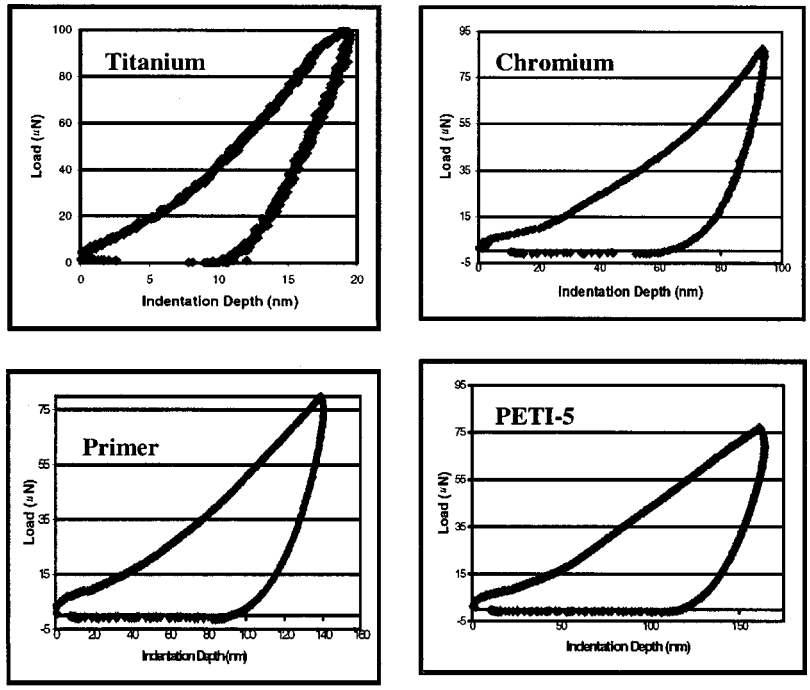

Figure 4 Load-Displacement curves of the characteristic curves of each material at the Titanium/Sol-gel/Primer/PETI-5 adhesive interface aged for 1000 hours.

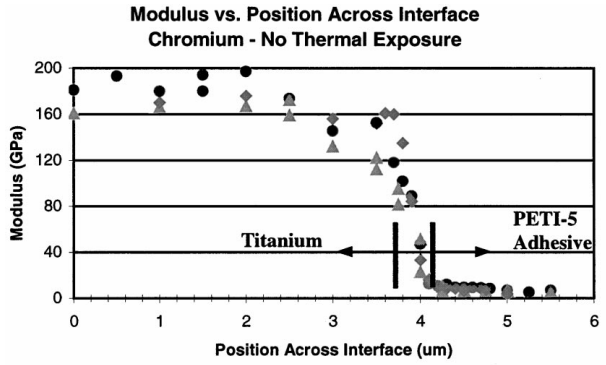

Figure 5 Modulus versus Position Across Interface (μm) of three measurements conducted transverse of 15-3-3-3 titanium/chromium/ BR-X5 primer/FM-X5 PETI-5 laminate and aligned to indicate modulus differences of each material.

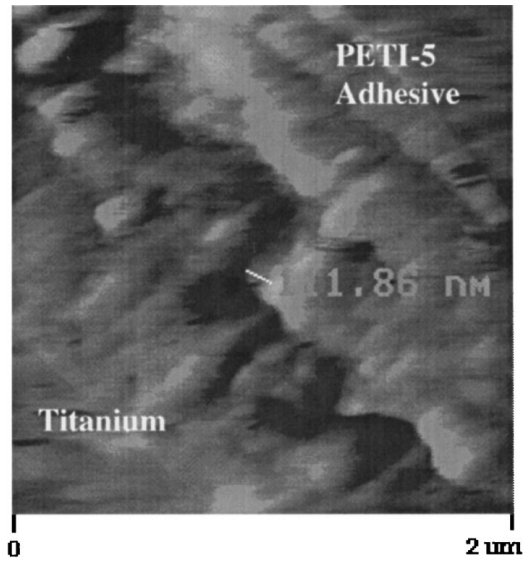

Figure 6 Friction force microscopy image of the Titanium – sol-gel – primer interface. The distance at the point depicted is 111.86 nm, well within the limits of the manufacturing process.

The complexity of the laminate interface adds difficulty in determining a consistent test procedure and analysis method. Generally, indentation results obtained across the laminate interface were shifted to compensate for the uneven profile at the interface. Multiplot presentations are adjusted to the PETI-5 polymer modulus allowing for the overlay of several experimental runs to be analyzed simultaneously.

As an example, Fig. 5 depicts three measurement sequences using a cube-corner diamond tip to indent across a Titanium 15-3-3-3, Chromium, BR-X5, FM-X5 laminate exposed to room temperature. The diamond tip is aligned to one side of the interface, as defined by an AFM image (Fig. 6), and traversed across the multi-material laminate interface at discreet steps at 100 nm or less (represented by the X-axis in Fig. 5). Tests were performed at a constant depth setting of 40 nm and many times more than one measurement was made at a particular transverse location across the laminate by moving the indenter tip 100 nm to one direction or the other on the interface.

Due to the uneven topography of the titanium substrates, there is difficulty in measuring multiple parallel transverse measurements across the interface. This is compounded with the process variations in both the primer application thickness and both the chromium and sol-gel thickness variations in each laminate. AFM images conducted in friction force mode to increase material resolution indicate the variation in the sol-gel and topographical discontinuity in the titanium substrate to be significant (Fig. 6). The point selected for measurement across the sol-gel interface is 111.86 nm, although

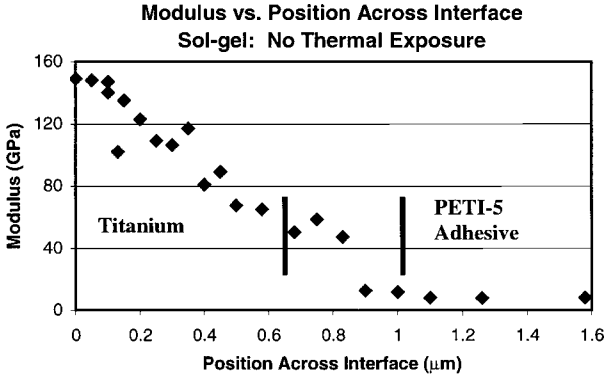

Figure 7 Modulus vs. Position across the Sol-gel, "No Thermal Exposure" laminate interface.

clearly the thickness varies across the laminate within this 2 μm $\times$ 2 μm image.

Therefore, when plotting multiple measurement sequences on one graph, the X-axis reads in nanometers and begins at zero, although this is arbitrary as these measurements are in a relative scale across the laminate. After several indentations are made, the series of modulus versus position values are plotted together and aligned to the inflection point between the PETI-5 Primer and coating interface. This position was selected because it is consistently the most accurate point in which to distinguish a modulus and hardness variation. This makes data interpretation difficult and forces a comparison with standards to insure accuracy of the alignment of multiple measurements. Modulus values from a single transverse indentation conducted across a sol-gel laminate in the "As Manufactured" condition is provided in Fig. 7. Load levels were kept at a constant load of 100 μN and thus indentation depths were between 30 nm for titanium up to 130 nm for PETI-5.

The distance between indentations were kept to 100 nm or less. In Fig. 7 one is able to view the modulus values of the titanium decline as it approaches the interface and the step-wise nature of each material modulus. Clearly, an edge effect exists in the titanium substrate. This could be due to the method by which the laminate was manufactured or perhaps the processing of the titanium itself. Stress relaxation at the edge could also account for the decrease in modulus as the edge of the laminate is approached. This trend exists in all titanium laminates tested, regardless of the thermal aging condition.

Modulus results of the sol-gel laminate indentation results reveal there is a similar change in the PETI-5 based polymer materials due to aging while the sol-gel polymer interface shows a degradation of approximately 20%. The plot in Fig. 8 illustrates three representative plots of the individual measurements and Table II summarizes the results of the measurements. Again, at least three measurements were conducted at each interface but in nearly all cases, several more than three were performed and the results were averaged to arrive at the values published in the tables.

A compilation of modulus results of several tests conducted across a chromium interface in the three conditions considered reveals that the affect of aging increases the modulus of the PETI-5 based primer and adhesive between 20–25%. While the effect on the chromium indicates a modulus increase of approximately 15% at 1000 hours, there is a minimal effect between 1000 and 2000 hours. Table III summarizes the corresponding modulus values.

TABLE II Modulus results as a function of aging: Sol-gel interface

Condition	Sol-Gel	Primer	PETI-5
As Manufactured	46–58 GPa	11–13 GPa	7–8.5 GPa
1000 Hours	58–63 GPa	13–15 GPa	8–10 GPa
2000 Hours	58–63 GPa	13–15 GPa	10–12 GPa

TABLE III Modulus results as a function of aging: Chromium laminate interface

Condition	Chromium	Primer	PETI-5
No Exposure	26–29 GPa	11–13 GPa	7–8.5 GPa
1000 Hours	32–36 GPa	13–14 GPa	8–10 GPa
2000 Hours	34–38 GPa	14–16 GPa	10–11 GPa

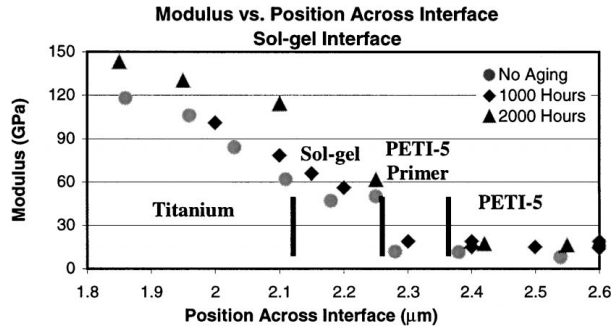

Figure 8 Modulus across laminate interface as a function of aging exposure: Sol-gel.

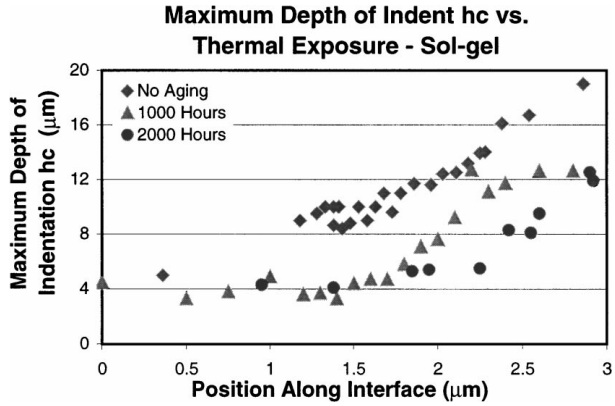

Figure 9 Maximum depth of indent h_c across sol-gel interface as a function of thermal exposure.

The measurement of h_c, defined earlier as the contact depth, may be referred to as a direct relationship to the plastic deformation of a material [18]. The h_c value for both the chromium and sol-gel interfaces has been determined as a function of environmental exposure. A sample of these measurements in the sol-gel systems as a function of aging are depicted in Fig. 9.

In each the maximum depth of the aged polyimide based primer and adhesive decreases by up to 50%,

indicting conclusively that chain embrittlement or shrinkage is associated with aging of the laminate. Note however that within the polymer, the depth of penetration increases as a function of distance from the titanium-coating hard surface and further into the bulk polymer, regardless of the aging condition. The relationship between the three aging conditions remain the same in both sample cases indicating that the trend is repeatable regardless of the coating system on the titanium substrate.

The reduction in contact depth of the PETI-5 adhesive, between 25% and 50%, corresponds to the reduction of Ti-6Al-4V/FM-5 strain energy release rate as a function of aging (27%), where it has been suggested this was due to the chemical aging/oxidation of the material system in air [9]. Strain energy release rate G is given by the following equation:

$$G = 9\Delta^2 \frac{\mathrm{EI}_{\mathrm{eff}}}{4B(a+x)^2} \tag{3}$$

where B is the specimen width, a is the crack length, x is the apparent crack offset, $\mathrm{EI}_{\mathrm{eff}}$ is the effective flexural rigidity, and Δ is the specimen opening displacement at the point of load application. The parameter $\mathrm{EI}_{\mathrm{eff}}$ is determined from slope of the specimen compliance as measured experimentally [9].

As a function of aging, polymeric embrittlement increases with chain rigidity resulting in a lower system free energy. As a result, the modulus increases with a corresponding decrease in system strain resulting in a contact depth decrease for an identical load and tip geometry. We interpret the modulus increase reported herein to correlate with the decrease in strain energy release rate G reported in Ref. 9. The reduction in strain energy release rate G is dominated by the decrease in the crack opening displacement term Δ (squared in the numerator) and is due primarily to the decrease in free energy (i.e., chain mobility) and lower polymer strain to failure. The polymer chain embrittlement results in a reduced strain and thus an increase the polymer modulus and correspondingly will result in a reduction in the PETI-5 strain energy release rate G.

Change in the modulus and depth of penetration of PETI-5 near the surface of the substrate is probably due to the constrained mobility of the polymer [19]. This may be seen in Figs 5 and 7 where the modulus decreases slightly in the PETI-5 (by approximately 1GPa) as a function of distance from the hard surface. The coated titanium influences the segmental mobility and relaxation in the polymer surface due to the adsorption interaction and conformation restriction imposed by the surface [20]. Additionally, polymer structure formation near a surface will be different from the bulk polymer due to the changes in molecular mobility. For instance, the density of a polymer near a surface is generally less than in the bulk due to the retardation of the relaxation process [21]. In conjunction there is usually a rise in the packing density for polymer molecules very close to a solid surface, possibly due to the orienting nature at the surface. It has been shown that the elastic modulus of a polymer increases with decreasing surface to volume ratio (i.e., distance to the surface) as a result of decreased chain mobility that influences the adhesion bond strength [22, 23].

4. Conclusions

High resolution, low-load indentations performed on titanium/chromium/PETI-5 primer/PETI-5 adhesive and titanium/sol-gel/PETI-5 primer/PETI-5 laminates proved to be very tip dependent. Sample preparation involved a significant amount of procedural development as the wear rate differential between both sol-gel and chromium coatings and PETI-5 impact dramatically the nature of the interface under shear conditions. Material standard measurements were necessary to achieve a high degree of confidence in the interpretation of the inhomogeneous nature of the interface.

Indentation studies of Sol-gel coated Titanium substrates indicate a pronounced step-wise interface continuing well into the Titanium laminate (3–4 μm). As compared to un-aged PETI-5 adhesive, aged material increased in modulus on average over 25% after 2000 hours at 204 °C, from 8 GPa to 11 GPa while the primer modulus increase was slightly under 15%.

Sol-gel increased in modulus after 1000 hours of exposure by approximately 15%, achieving a plateau at this level and showing no additional signs of modulus deviation with additional aging. Chromium behaved in a different manner. Initially, the un-aged material maintained an average modulus of 27.5 GPa, approximately half that of the sol- gel. More importantly, the modulus gradually rose with aging, rising approximately 25% as a function of aging up to 2000 hours with no plateau visible within the upper limits of the time duration of this study.

The analysis of the maximum indentation depth h_c indicates that both laminate configurations exhibit up to a 50% decrease in plastic deformation at the PETI-5 primer/PETI-5 adhesive areas as a function aging, indicating a decrease in chain mobility, additional polymer embrittlement, and loss of ductility. It is clear that further testing is necessary to confirm the observations reported herein and that a more comprehensive database must be developed that addresses additional environmental conditions such as moisture, hot-wet conditions, and longer periods of severe environmental exposure.

These results indicate the mechanisms that determine the mechanical performance of complex multimaterial structural composites may be analyzed at the nanoscale level and reveal information critical to the long-term system performance. In addition, strain rate sensitivity at the nanoscale, not addressed in this study, could provide additional insight to the overall system performance.

Acknowledgements

We wish to express our gratitude to the Boeing Company and to the National Aeronautics and Space Administration for their generous support for this study (High Speed Research Program, NAS1-20220). We thank the NASA CAS ITD Team, NASA Langley Research Center, for the review of this document and

Mr. Kevin Pate, HSCT Materials & Processes, The Boeing Company, for his patience and guidance during this effort. In addition, we wish to thank Dr. Van Eden, ESR Scientific, Hannesville, WA, and Mr. Hanson Fong of the University of Washington, Bioceramics Laboratory, for their assistance. We further acknowledge the Boeing Company for providing assistance in sample preparation (Mr. Luther Gammon) and obtaining a portion of the SEM images.

References

1. A. FALCONE, K. D. PATE, T. Q. CAO, G. F. HSU and M. E. ROGALSKI, in Proc. 41st Int. SAMPE Sym. (1996) p. 1035.
2. J. G. SMITH and P. M. HERGENROTHER, *Poly. Prepr.* **35** (1994) 353
3. M. R. ALLEN, NASA-CR-198193 (1995).
4. A. J. KINLOCH, *J. Adhesion* **10** (1979) 193.
5. H. R. DAGHYANI, L. YE and Y. W. MAI, *J. Mater. Sci.* **31** (1996) 2523.
6. J. F. WATTS, J. E. CASTLE and T. J. HALL, *J. Mater. Sci. Lett.* **31** (1988) 2523.
7. J. Z. WANG, H. PARVATAREDDY, T. CHANG, N. IYENGAR, D. A. DILLARD and K. L. REIFSNIDER, *Comp. Sci. Tech.* **54** (1995) 405.
8. J. L. SULLIVAN, E. J. BLAIS and D. HOUSTON, *ibid.* **47** (1993) 289.
9. H. PARVATAREDDY, J. G. DILLARD, J. E. McGRATH and D. A. DILLARD, *J. Ad. Sci. Tech.* **12** (1998) 615.
10. W. W. GERBERICH, J. C. NELSON, E. T. LILLEODEN, P. ANDERSON and J. T. WYROBEK, *Phil. Mag. A* **74** (1996) 1117.
11. S. I. BULYCHEV and V. P. ALEKHIN, *Zavod. Lab.* **41** (1975) 1137.
12. M. F. DOERNER and W. D. NIX, *J. Mat. Res.* **1** (1986) 601.
13. W. C. OLIVER and G. M. PHARR, *ibid.* **7** (1992) 1564.
14. K. L. JOHNSON, "Contact Mechanics" (Cambridge University Press, 1989).
15. W. W. GERBERICH, W. YU, D. KRAMER, A. STRIJNY, D. BAHR, E. LILLEODDEN and J. NELSON, *J. Mat. Res.* **13**(2) (1998) 421.
16. S. P. BAKER, in Nanoindentation Aspects, Tutorial Notes, MRS Spring 1998 Meeting, Symp. T-Tutorial.
17. L. M. GAMMON and D. J. RAY, in Proc. 30th IMS Conv., Seattle, WA, July 20–25, 1997.
18. H. F. WANG, J. C. NELSON, W. W. GERBERICH and H. E. DEVE, *Acta Metall. Mater.* **42**(3) (1994) 695.
19. J. D. MILLER and H. ISHIDA, in "Fund. of Ad.," edited by L. H. Lee (Plenum Press, 1992) p. 291.
20. Y. A. LIPATOV, *Rubber Chem. Tech.* **49** (1976) 1311.
21. *Idem., Trans. Int. Plast. Ind.* **4** (1966) 83.
22. *Idem., Polymer* **16** (1975) 582.
23. Y. S. LIPATOV and V. BABICH, *Vysokomol Soedin.* **10** (1968) 848.

Received 22 November 1999
and accepted 14 August 2000